Determination of Lunar Ilmenite Abundances
From Remotely Sensed Data

J. R. Johnson, S. M. Larson, and R. B. Singer

Department of Geosciences/Lunar and Planetary Laboratory

The University of Arizona

Abstract

The mapping of ilmenite on the surface of the Moon is a necessary precursor to the investigation of prospective lunar base sites. Telescopic observations of the Moon using a variety of narrow bandpass optical interference filters are being performed as a preliminary means of achieving this goal. Specifically, ratios of images obtained using filters centered at 0.40 μm and 0.56 μm provide quantitative estimates of TiO_2 abundances. Analysis of preliminary distribution maps of TiO_2 concentrations allows identification of specific high-Ti areas. Investigations of these areas using slit spectra in the range 0.30–0.85 μm are underway to search for discrete spectral signatures attributable to ilmenite.

Introduction and Background

An important criterion during selection of lunar base sites will be the availability of ilmenite ($FeTiO_3$) for use as a local resource. The distribution of ilmenite across the surface of the Moon must therefore be well known. Earth-based telescopic remote sensing of the lunar surface in combination with laboratory spectral reflectance measurements of returned lunar samples has proven to be a valuable tool, both in discerning relative differences between lunar material and in establishing more quantitative estimates of surface compositions (e.g., Head et al. 1978).

Lunar ilmenites most often contain greater than 50 wt% titanium dioxide (TiO_2), making ilmenite the dominant titanium-bearing mineral on the surface of the Moon. Surface distribution maps of TiO_2 abundances are consequently valuable in determining regions of probable high-ilmenite concentrations.

Charette et al. (1974) measured TiO_2 contents of sampled bulk lunar soils and compared their spectral reflectivities in the laboratory. An empirical relation between weight percent TiO_2 and the reflectance slope between 0.40 μm and 0.56 μm was established (Figure 3.1). The slope of the lunar reflectance spectrum in this region is primarily affected by the absorptions due to Fe and Ti in the lunar soil, i.e., the agglutinates and glasses. The relation is therefore more accurate for mature soils (those that have been extensively reworked by micrometeorite impacts), particularly in the lunar maria. Charette et al. also found the relation to hold for telescopic spectra of lunar landing sites (Figure 3.2).
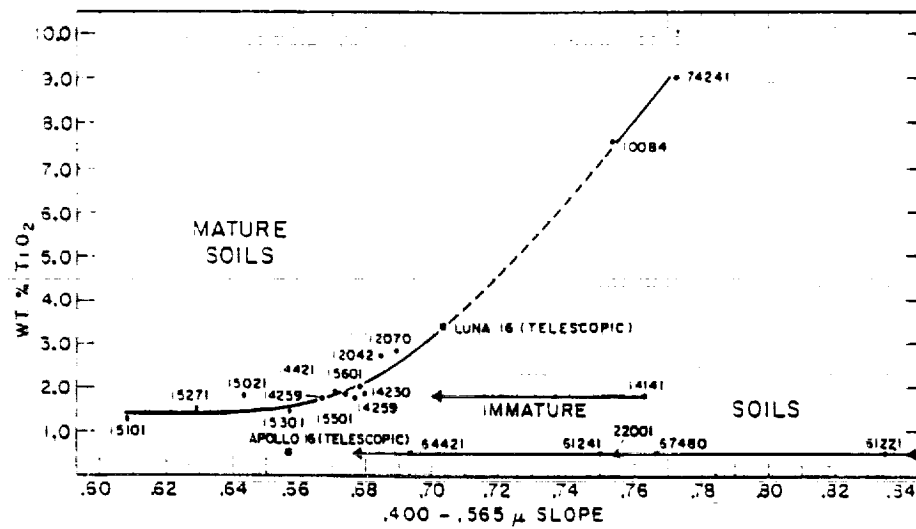
Figure 3.1   Plot of TiO_2 percentage of the bulk lunar soils as a function of 0.40 μm to 0.56 μm slope. (From Charette et al. 1974.)
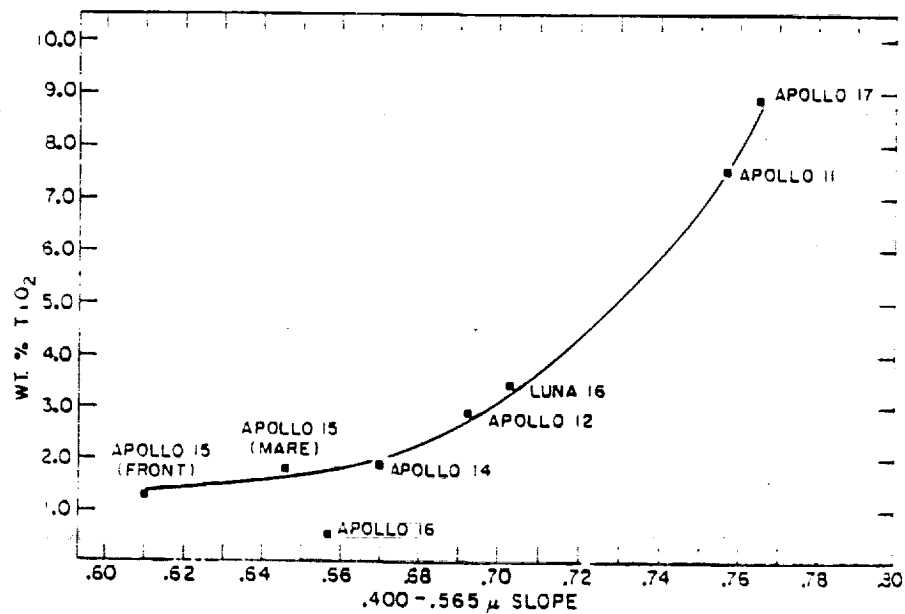

Figure 3.2   Plot of TiO_2 percentage versus 0.40 μm to 0.56 μm slope for telescopic spectra. The TiO_2 contents of telescopic areas are averages of sampled soils used in Figure 3.1. (From Charette et al. 1974.)

Johnson et al. (1977) used a silicon vidicon imaging system to obtain multispectral images of the Moon through narrow bandpass interference filters centered at 0.38 μm and 0.56 μm. An abundance map of TiO_2 for the northern maria was produced by converting the 0.38/0.56 μm ratio (normalized to a standard area in Mare Serenitatis named MS-2) to weight percent TiO_2 (Figure 3.3).

Figure 3.4 shows the most recent version of the relation between the 0.40/0.56 μm ratio and weight percent TiO_2 (Pieters 1978). At values of TiO_2 less than about 4 wt%, the absorbing effects of the Ti-Fe opaque phases can be obscured by the effects of other contaminants such as Fe-metal, plagioclase, and non-opaque (homogeneous) glass compositions in the soil. Thus, a ratio value of 1.00 may correspond to a range of 0-2.5 wt% TiO_2.

Multispectral Image Acquisition and Results

Previous efforts to obtain multispectral images of the Moon used television-type silicon vidicon tubes (e.g., McCord et al. 1976, 1979). These images possessed spatial resolutions of about 2 km per picture element (pixel) but covered relatively small areas on the lunar surface. Mosaicking of photographs taken of the individual vidicon images was necessary to achieve greater areal perspective. Contrast differences between the mosaic frames suffer from some uncertainties, which discourage comparison of apparently similar gray-level intensities between frames not contiguous.

Newer imaging technologies use charge-coupled device (CCD) systems that provide better stability and higher photometric precision. For our project, an RCA 320 × 512-pixel CCD chip has been used at The University of Arizona Tumamoc Hill Station 0.5-m telescope. In October 1989, multispectral images of the Moon were obtained at the f/4 Newtonian focus using a variety of narrowband interference filters (Table 3.1). In addition to the 0.40 μm and 0.56 μm filters, ultraviolet filters were used to discern reflectance differences in that interesting but seldom-imaged portion of the lunar spectrum. The near-infrared filters can be used to investigate additional surface properties; for example, the 0.95/0.56 μm ratio can be used as a relative indicator of surface maturity (McCord et al. 1976).

Five images are necessary to cover the full Moon (Figure 3.5). The spatial resolution of the images is about 5.3 km per pixel on the Moon. Figure 3.6 shows four of the image ratios obtained by dividing the 0.40 μm images by the 0.56 μm images in which the brighter areas correspond to higher ratio values. Full-size versions of the 0.40 μm image and 0.40/0.56 μm ratio for the eastern section of the Moon are shown in Figures 3.7 and 3.8. Using an average of the plot in Figure 3.4 (dotted line) to calibrate
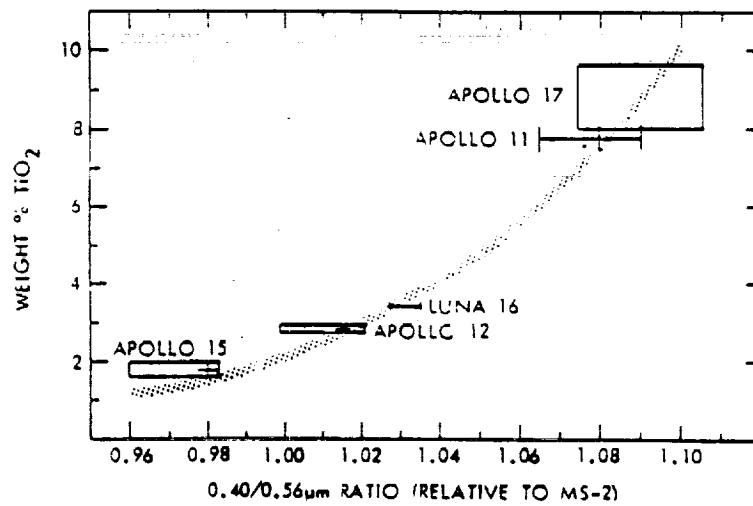
Figure 3.3   Weight percent TiO_2 versus 0.40/0.56 μm ratio (relative to MS-2). (From Pieters and McCord 1976.)
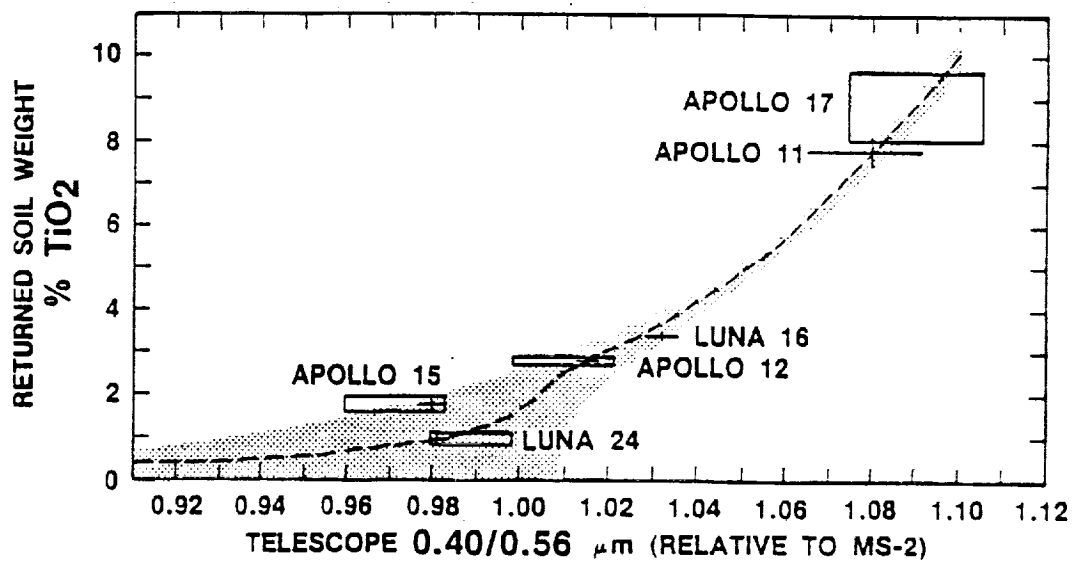

Figure 3.4   Relationship between weight percent TiO_2 in lunar mare soils and the the 0.40/0.56 μm ratio for telescopic spectra relative to MS-2. The stippled area is the estimated range of TiO_2 that can be derived from a 0.40/0.56 μm ratio measurement of mature mare regions. Dotted curve approximates the curve used for calibration of ratio values to wt% TiO_2 in present study. (After Pieters, 1978.)
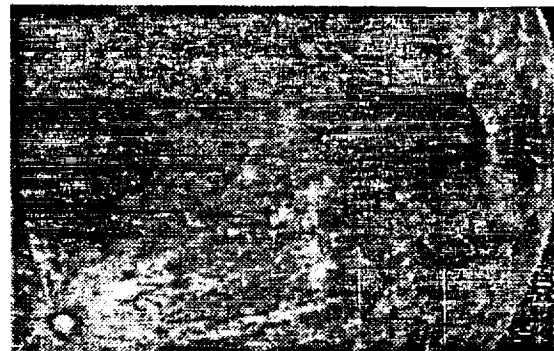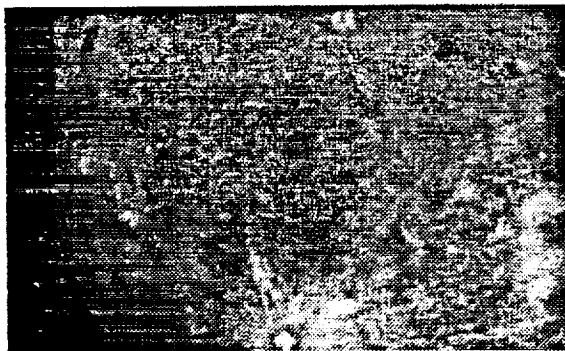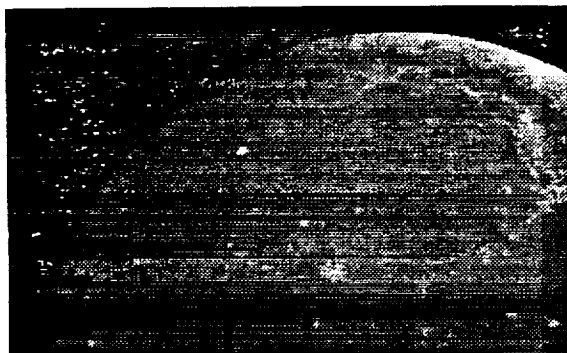
ORIGINAL PAGE
BLACK AND WHITE PHOTOGRAPH

Figure 3.5   Images of the Moon obtained with bandpass interference filter centered at
0.40 μm. (Reduced-size postscript laser printer copies.)

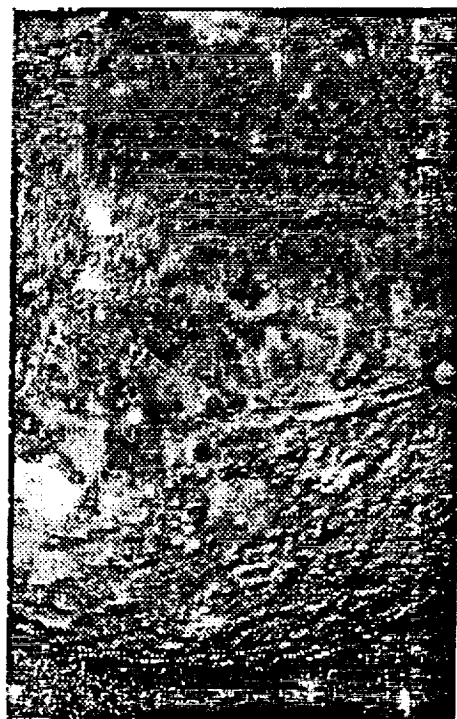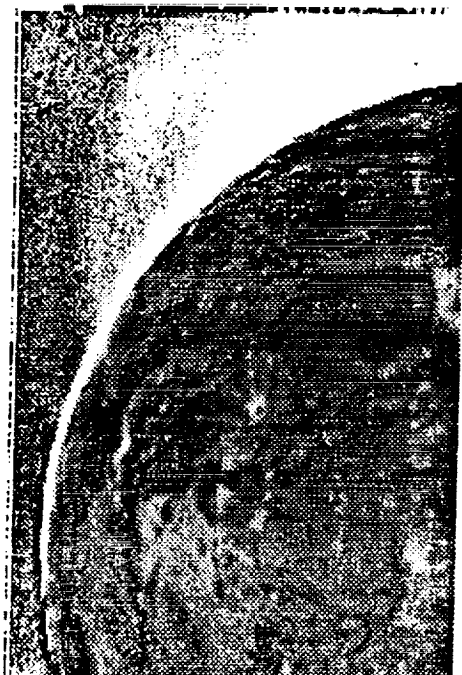ORIGINAL PAGE
BLACK AND WHITE PHOTOGRAPH

Figure 3.6   Preliminary 0.40/0.56 μm ratio images of the moon.   (Reduced-size postscript laser printer copies.)

ORIGINAL PAGE
BLACK AND WHITE PHOTOGRAPH

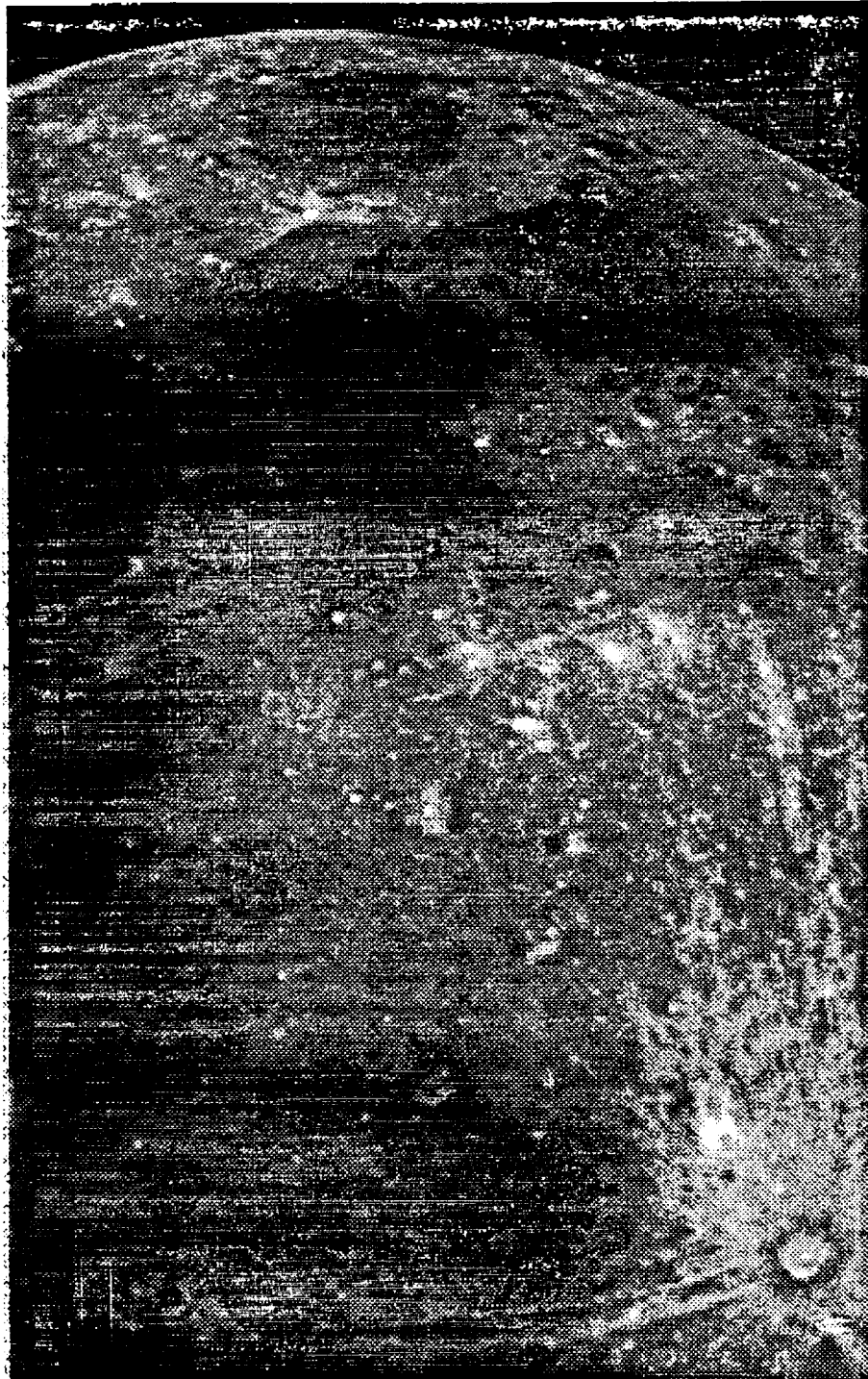
Figure 3.7   Image of eastern section of Moon taken through 0.40 μm filter.   (Full-sized postscript laser printer copy).

ORIGINAL PAGE
BLACK AND WHITE PHOTOGRAPH

Figure 3.8   Preliminary 0.40/0.56 μm ratio image of the eastern section of the moon. (Full-sized postscript laser printer copy.)

Table 3.1   Bandpass interference filters.

Center Wavelength (nm)	Bandwidth [FWHM] (Å)
309	75
319	102
338	106
365	80
389	48
400	95
427	80
560	95
729	128
902	289
948	184

images, a TiO_2 wt% abundance map can be constructed (Figure 3.9). The value for MS-2 was taken from the eastern ratioed image section in Figure 3.8.

Variability in observed TiO_2 concentrations in some overlapping areas between adjacent image ratio sections rarely exceeds 2 wt% but is nevertheless problematic. Investigations are underway to calibrate the MS-2 standard to areas common to the overlapping portions of individual images in order to provide a standard ("tied" to MS-2) for those images in which MS-2 is not in view.

Spectroscopic Studies

Those areas highest in TiO_2 content (as determined from analysis of the preliminary maps of TiO_2 concentration) are being studied spectroscopically as well. Initial attempts were made in November 1989 (again at Tumamoc Hill) to obtain slit spectra for several regions of interest using the CCD spectrograph/camera designed by one of us (S.M.L.). It includes two blue-blazed gratings, one giving a spectral range from 0.30 μm to about 0.88 μm with 11 Å per pixel and the other providing spectra from 0.30 μm to about 0.56 μm at 5 Å per pixel. The 6 × 0.2 mm slit used corresponded to 130.0 × 4.3 km on the Moon. In December 1989, further spectra were obtained using a 20 × 0.25 mm slit with the spectrograph, corresponding to 442.3 × 5.5 km on the Moon. For the December run, a new reflecting slit allowed the image of the spectrographic slit on the Moon to be simultaneously videotaped for all lunar spectra so that the precise region being analyzed could be recorded accurately.

For both the November and December observations, each spectral observation was followed immediately by acquisition of spectra for the MS-2 area. In this way, relative reflectance spectra (ratioed to MS-2) free from instrumental and atmospheric effects were collected.

Figure 3.9 TiO_2 abundance map of the eastern section of the Moon based on 0.40/0.56 μm ratio image. Dark gray areas correspond to <5 wt %. Light gray areas correspond to 5-8 wt%. Brightest areas correspond to >8 wt%.

Figure 3.10 shows relative reflectance plots obtained in December with the lower resolution grating for four lunar areas. The spectra have been normalized to unity at 5600 Å. The Tranquillitatis and Iridium mare regions show a characteristic upturn in slope toward the near-UV and a noticeable upturn in the near-IR (longward of about 7800 Å). From preliminary maps, Tranquillitatis was shown to have larger TiO_2 concentrations than Iridium. The relative reflectance spectra are consistent with this comparison, as the slope of the spectrum for Tranquillitatis is steeper than that for Iridium, i.e., Tranquillitatis has a greater 0.40/0.56 μm ratio and a corresponding higher TiO_2 value (Figure 3.4). For comparison with mature mare areas, the craters Tycho (located in the southern highlands) and Aristarchus (located in northern Oceanus Procellarum) show a more constant relative reflectance in the near-UV and a steady decrease toward the near-IR. These two spectra also exhibit an abrupt downturn in relative reflectance at about 4800 Å

The relative reflectance spectra can be more readily compared to laboratory spectral reflectance measurements of lunar soils by calibrating them to absolute reflectance. In order to accomplish this, further spectra were obtained at The University of Arizona Catalina Observatory 1.54-m telescope in January 1990. Spectra were recorded for a solar analog star (i.e., one with spectral characteristics indistinguishable from the Sun) and then ratioed to spectra of the MS-2 region for the same air mass in order to provide an absolute spectrum for MS-2. This can be applied to the December relative reflectance ratios in order to provide absolute reflectance spectra for specific lunar areas. Reduction of the spectra to this form is presently underway.

Conclusions

The multispectral image data set taken in October 1989 is of sufficient quality to be used for analysis of both TiO_2 variations in the lunar maria and relative maturity differences of the lunar surface. Initial results from the October images show most of western Mare Tranquillitatis to be a region of high TiO_2 concentrations (>8 wt%) (Figure 3.10); this region is being investigated more fully with high-resolution spectra. Other smaller areas that show high concentrations, such as the "dark spots" east of the crater Copernicus and in the region of Sinus Aestuum (south of Mare Imbrium), are also under spectral scrutiny.

The 0.95/0.56 μm maturity index may be of interest to other SERC investigators when used in conjunction with the TiO_2 abundance map. M. Hutson, J. Ruiz, and J. Lewis conclude that high-Ti soils with low agglutinate content (immature soils) are best for processing and separation of ilmenite grains. T. Swindle and C. Glass note that the
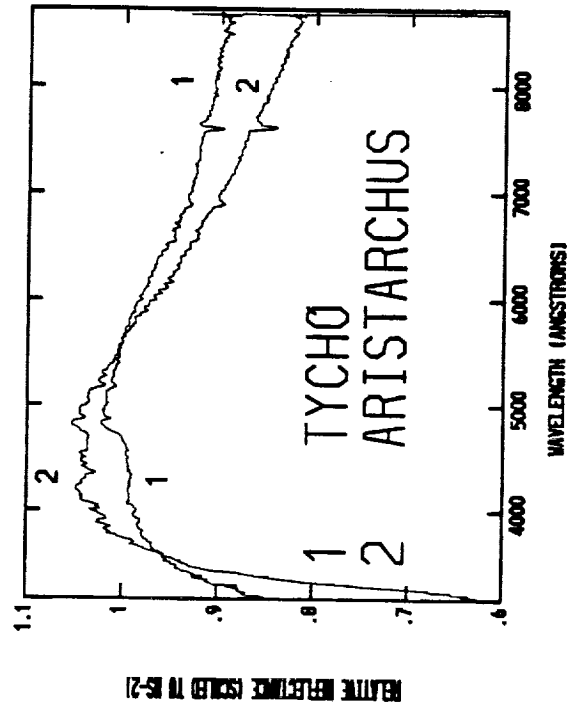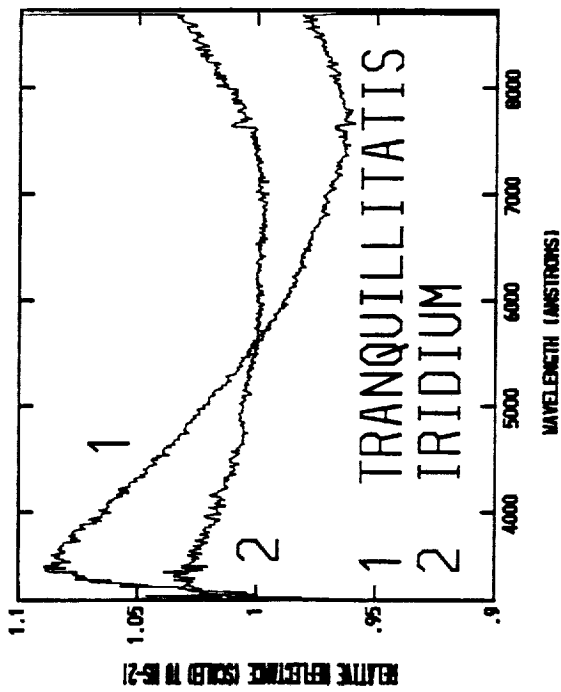
TRANQUILLITATIS
IRIDIUM
1
2

TYCHO
ARISTARCHUS
1
2

Figure 3.10   Relative reflectance spectra scaled to MS-2 and normalized to unity at 5600 Å The relative reflectance for Iridium (a large flooded crater in northern Mare Imbrium) shows a shallower slope in the 4000-5600 Å region than does the spectrum for western Mare Tranquillitatis. The craters Tycho (in the highlands) and Aristarchus (in Oceanus Procellarum) are shown for comparison.

highest Ti soils are apparently the best sites for ^{3}He implantation. Since ^{3}He will be more abundant in soils that have been long exposed to the solar wind, they prefer high-Ti soils with abundant agglutinates (mature soils).

Final products of this project will be TiO_2 abundance maps of the entire lunar near-side maria. Other ratio images [including the relative maturity index (0.95/0.56 μm)] may be of enough interest in comparison with each other to warrant additional analysis. Qualitative analysis of relative and/or spectral reflectance measurements of several areas will provide further details regarding the mineralogical and chemical makeup of high-Ti regions. The Apollo 15 and 16 orbital gamma-ray data set for titanium is also being used as an additional resource. Comparisons of the two methods' estimates of Ti concentrations will give further insight to the precision of the spectral studies.

References

Charette, M. P., McCord, T. B., Pieters, C., and Adams, J. B., 1974, "Application of Remote Spectral Reflectance Measurements to Lunar Geology Classification and Determination of Titanium Content of Lunar Soils," *J. Geophys Res.*, Vol. 79, p. 1605.

Head, J. W., Pieters, C., McCord, T., Adams, J., and Zisk, S., 1978, "Definition and Detailed Characterization of Lunar Surface Units Using Remote Observations," *Icarus*, Vol. 33, pp. 145-172.

Johnson, T. V., Saunders, R. S., Matson, D. L., and Mosher, J. A., 1977, "A TiO_2 Abundance Map for the Northern Maria," *Proc. Lunar Sci. Conf. 8th*, pp. 1029-1036.

McCord, T. B., Pieters, C., and Feierberg, M. A., 1976, "Multispectral Mapping of the Lunar Surface Using Groundbased Telescopes," *Icarus*, Vol. 29, pp. 1-34.

McCord, T. B., Grabow, M., Feierberg, M., Maclaskey, O, and Pieters, C., 1979, "Lunar Multispectral Maps: Part II of the Lunar Nearside," *Icarus*, Vol. 37, pp. 1-28.

Pieters, C. and McCord, T. B., 1976, "Characterization of Lunar Mare Basalt-Types: Luna 24 Landing Areas as Derived From Remote Observations," *Geophys. Res. Lett.*, Vol. 3, pp. 697-700.

Pieters, C., 1978, "Mare Basalt Types on the Front Side of the Moon: A Summary of Spectral Reflectance Data," *Proc. Lunar Planet. Sci. Conf. 9th*, pp. 2825-2849.